Surface morphology-controlled poly(ε-caprolactone) nanofiber anti-fouling coating: A promising approach for marine applications

Journal of Physics: Conference Series **2873** (2024) 012046 doi:10.1088/1742-6596/2873/1/012046

Surface morphology-controlled poly(ε-caprolactone) nanofiber anti-fouling coating: A promising approach for marine applications

Fengqin Li, Yuxue Hu, Dongpo Zhu and Guizhong Tian*

College of Mechanical Engineering, Jiangsu University of Science and Technology, Zhenjiang, ZIP 212100, China

*Corresponding author's e-mail: justtgz@163.com

Abstract: To effectively combat marine biofouling, biomimetic anti-fouling coatings have garnered widespread attention as a novel anti-fouling method. Based on this biomimetic concept, this study adjusted the electrospinning process parameters and selected different solvent systems to effectively modify the surface morphology of poly(ε-caprolactone) (PCL) nanofiber coatings, developing a non-toxic anti-fouling smooth surface. These biodegradable slippery liquid-infused porous surfaces (SLIPS) coatings offer a simple way to prepare maritime anti-fouling coatings in an eco-friendly manner. They can withstand a variety of liquid, material, and microbiological contaminations.

1.Introduction

Marine biofouling is a rapid and intricate process that extensively impacts the sustainable development of human activities in marine industries and maritime transportation[1,2]. Researchers have developed various anti-fouling methods, such as physical[3], chemical[4], and biological antifouling[5]. There are disadvantages to both physical and chemical approaches in terms of affordability, environmental friendliness, and stability. Biological anti-fouling methods draw inspiration from natural organisms' anti-fouling behaviors and employ non-toxic strategies to prevent organism attachment. This approach holds promise to replace currently widely used anti-fouling coatings containing toxic organotin compounds, presenting broad application prospects[6].

Inspired by the pitcher plant, this study injects lubricants into porous substrates to form a thin liquid film on the surface, achieving liquid-liquid repellence instead of liquid-solid interface adhesion. Utilizing electrospinning technology, porous nanofiber coatings are fabricated using biodegradable elastomeric polymer (poly ε-caprolactone, PCL). By adjusting electrospinning process parameters and selecting different solvent systems, the surface morphology of PCL nanofiber coatings is effectively tuned to improve surface roughness and hydrophobicity. Harmless lubricants are chosen for injection into the porous nanofiber matrix to realize exceptionally smooth characteristics. The entire fabrication process is efficient and kind to the environment, opening up a new avenue for the preparation of biodegradable nanofibers with potential applications in biomaterials and marine anti-fouling.

2. Experimental section

2.1. Materials

Poly ε-caprolactone (PCL, Mn = 8w~10w), dichloromethane (DCM, ≥99.5%, containing 50-150ppm isoprene stabilizer), N, N-dimethylformamide (DMF, AR, 99.5%), 100 mPa·s dimethyl silicone oil, and ethanol were all purchased from Shanghai Aladdin Bio-Chem Technology Co., Ltd. No additional changes were made to any of the materials. The Shanghai Collection Center for Bioresource Technology provided the Escherichia coli (E. coli, ATCC 25922).

2.2. Preparation of PCL nanofiber membrane

First, PCL was dissolved in a 1:1 mixture of main solvent DMF and cosolvent DCM. Each spinning solution and subsequent fiber membrane was represented by PCL8%, PCL10%, PCL12%, and PCL15%. Subsequently, PCL was dissolved in a homogeneous solution of main solvent dichloromethane (DCM) and cosolvent ethanol. The resulting spun fiber membrane was denoted as P-PCL8%. After 20 minutes of electrospinning, all electrospun fiber membranes were placed in a vacuum oven at 35°C for 24 hours to remove residual solvents. For specific spinning solution formulations and spinning processes, please refer to Table 1.

Table 1. Preparation formula and electrospinning process parameters.

Samples	Spinning solution formula			Electrospinning parameters			
	PCL (g/mL)	Solvent (v/v, mL)	Concentrations （Wt%）	Voltage (kV)	Distance between needle and collector (cm)	Injection speed (mL/h)	High shaft speed (mL/h)
		DCM/DMF					
PCL8%	0.08	4.5:4.5	8	18	10	2.5	100
PCL10%	0.1		10				
PCL12%	0.12		12				
PCL15%	0.15		15				
		DCM/Ethanol					
P-PCL8%	0.08	9.1:0.1	8				

2.3. Impregnation with lubricating oil

The prepared nanofiber membranes were immersed in 100 mPa·s dimethyl silicone oil for 10 minutes, followed by placement on a Büchner funnel for 1 hour to remove excess lubricant. The PCL and porous PCL membranes after impregnation with dimethyl silicone oil were referred to as SLIPS-1 and SLIPS-2, respectively.

2.4. Characterization

With the use of a Hitachi SU8600 cold field emission scanning electron microscope, the morphology of the electrospun fibers was examined. A contact angle goniometer (Theta Lite, BIOLIN Shanghai, China) was used to measure the static contact angle of 5 μL deionized water droplets on the coated surface at room temperature. The sliding angle (SA) was recorded using the drop and tilt method. A 100 mPa·s lubricating oil evaporation loss test was used to assess the lubricating oil's storage stability, and the sample weight loss was used to compute the lubricating oil evaporation loss.

2.5. Drag reduction experiments

In the drag reduction measurement experiments, a parallel plate rheometer (MCR92, Anton Paar, Austria) was employed to simulate the splashing of droplets on the surface (SLIPS). The top sensor of the rheometer was connected to a rotor with a diameter of 26 millimeters, which applied shear stress to the

fluid by rotating. The samples were securely attached under the rotor using adhesive. The gap between the rotor and the surface was maintained at a constant 0.5 mm.

2.6. Antibacterial adhesion resistance test

Using the agar plate method, the quantitative study of bacterial adherence on the coated surface was carried out. A constant temperature shaking incubator was employed to simulate the fluid environment, with Escherichia coli (ATCC 25922) chosen as the typical fouling test strain. Agar plate pictures of bacterial colonies were counted and analyzed to assess the coatings' short-term dynamic fouling resistance. The coverage of Escherichia coli on the coated surface was compared using ImageJ software.

3. Results and discussion

3.1. Surface morphology of PCL electrospun coating

SEM images in Figure 1 (a-d) depict the morphological evolution of electrospun PCL at different concentrations. At a PCL concentration of 8%, SEM revealed nanofibers with a diameter of approximately 150 ± 10 nm (Figure 1a). The average fiber diameter showed a rising trend from 8% to 15% of PCL content, which made them more prone to fusion (Figure 1d). Due to the minimal structural defects observed on the surface of PCL8% and the potential enhancement in hydrophobicity with finer fiber diameters[7], 8% PCL was chosen for further investigation.

Figure 1 (e) illustrates the morphology of electrospun PCL with ethanol as the guest solvent. On the PCL fibers, honeycomb-like pores are visible, which are caused by non-solvent-induced phase separation (NIPS). Ethanol moves to the droplet surface as DCM, which has a boiling point of about 39.8°C, evaporates first. When there is no solvent present, NIPS happens all the time and produces rich and poor phases. After the ethanol completely evaporates, the poor phase ethanol starts to nucleate and develop on the droplet surface, eventually producing holes. We have developed a simple and effective method, namely guest solvent-assisted electrospinning, to prepare uniformly porous PCL nanofibers with controlled surface morphology, which is crucial for designing surfaces for stable liquid infusion.

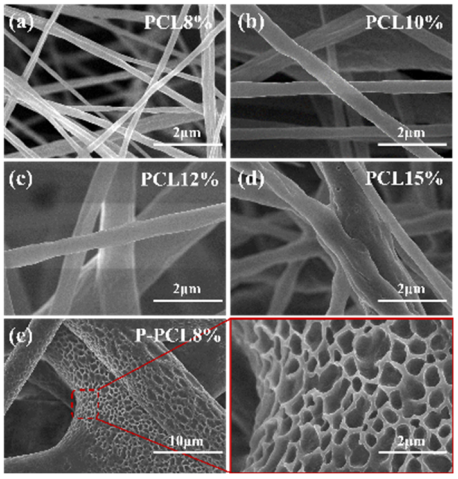

Figure 1. (a-d) SEM images of electrospun PCL membranes at different concentrations. (e) SEM image of porous PCL fibers electrospun from a guest solvent (ethanol) solution.

3.2. Wettability and slipperiness

Figure 2a presents the results of water contact angle (WCA) tests for different coatings. Among all electrospun PCL fiber mats, the WCA of the PCL mat obtained from an 8% PCL solution is the highest (~132°). As the concentration of the PCL solution increases, the WCA gradually decreases. It is well known that, in addition to hydrophobicity, the construction of a rough surface promotes hydrophobicity. The fibers produced from the 8% PCL solution in electrospinning typically exhibit the finest fiber diameter and often form rough surfaces with numerous interconnected pores, leading to improved

hydrophobicity. Based on the 8% PCL fiber mat, we obtained a WCA value of approximately 136° for P-PCL8%, which represents further improvement compared to the PCL8% coating. We speculate that the formation of porous fibers further increases the surface roughness, consistent with the SEM imaging results.

Subsequently, we injected lubricating oil into these PCL nanofiber membranes, and the silicone oil droplets readily spread over the mat surface (θ≈0°) and penetrated into the grid. To test the coating's slip performance, we conducted water droplet roll-off tests on the SLIPS-1 coating. The water droplet (~3μL) smoothly rolled off the oil-injected coating surface with a low sliding angle (<10°) (Figure 2b), demonstrating robust sliding behavior. This suggests that by filling the coating entirely by capillary action, the lubricating oil forms a full lubricating film that covers the substrate surface, greatly limiting later marine bacterial adherence[8].

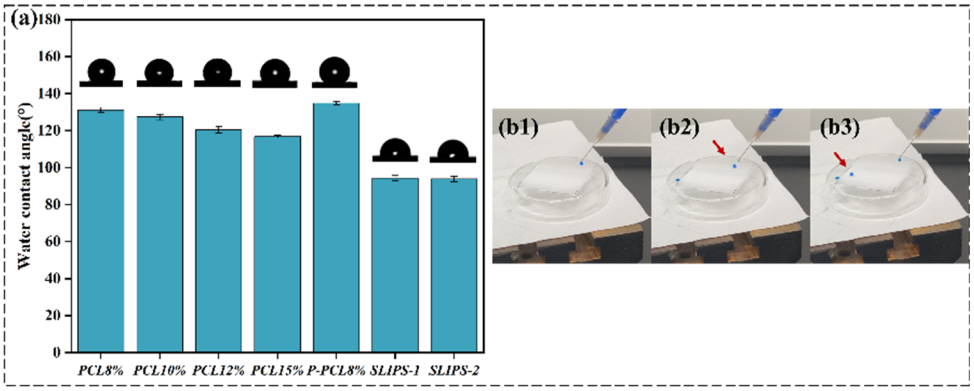

Figure 2. (a) Water contact angles (WCA) on different coating surfaces; (b) Water droplet roll-off test on oil-injected PCL8% electrospun coating.

3.3. Storage stability of lubricant

All of the SLIPS coatings demonstrated a decrease in oil film mass with time in the accelerated lubricant evaporation experiment (Figure 3), particularly in the first eight hours. This initial decline may be due to the instability of the surface oil film. The loss of oil film mass for each SLIPS coating slowed significantly after 8 hours. Notably, during the 48-hour oven experiment, PCL8% exhibited a faster decrease compared to P-PCL8%. SLIPS-2 showed a 7.85% lower rate of lubricant mass loss compared to SLIPS-1, suggesting that the porous fiber structure may enhance lubricant retention.

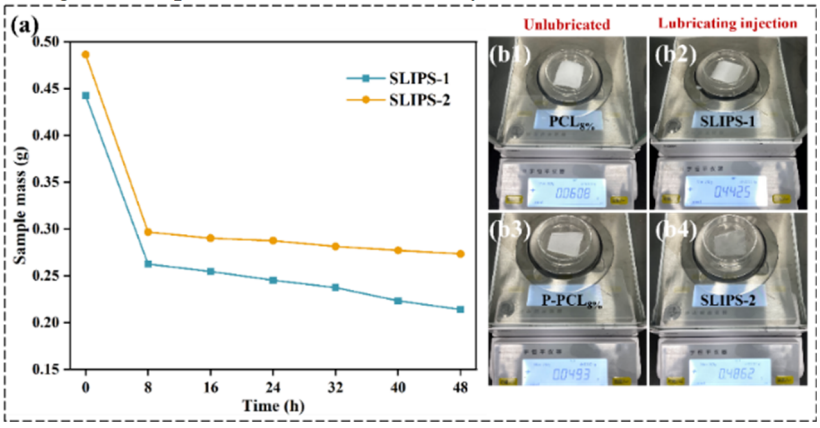

Figure 3. (a) Quality changes of SLIPSs coating at constant temperature at 50°C for 48 h.(b) Quality images of each coating.

3.4. Drag reduction performance of the sample

The drag reduction performance of the SLIPSs sample coatings was determined using a rheometer. The

experimental setup is illustrated in Figure 4 (a1-a3), where the SLIPSs sample coatings were affixed to glass dishes on the bottom plate, with a torque of 11.5±0.4 ~ 32.4±0.4 μN m applied to the reference copper substrate. The surface tension and viscosity of the measured lubricant were 20.5 mN/m and 100 mPa·s, respectively.

As depicted in Figure 4 (b), shear stress was directly proportional to shear rate. On the rheological curve, this material exhibited a straight line passing through the origin, with the slope representing its viscosity. From the perspective of shear thinning, apparent viscosity decreased with increasing shear rate (Figure 4 (c)). On the rheological curve, this was manifested by a decrease in slope with increasing shear rate, indicating that the fluid became more flowable at higher shear rates. The relationship between shear rate and drag reduction rate is presented in Figure 4 (d), where the drag reduction rate of SLIPS-1 approached 65%, and that of SLIPS-2 showed an enhancement of approximately 5% compared to SLIPS-1. Both oil-injected coating surfaces exhibited excellent drag reduction performance.

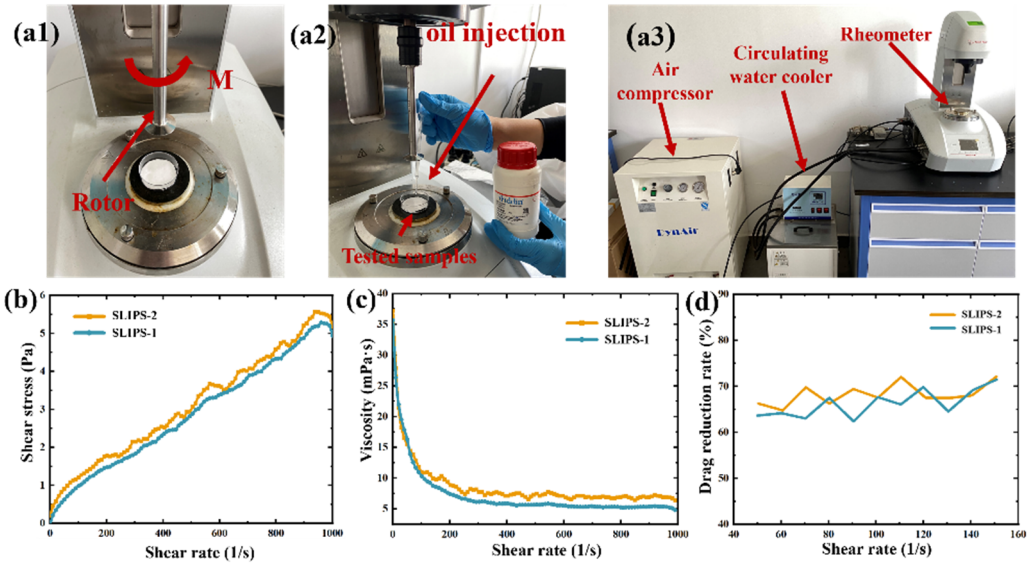

Figure 4. (a) Schematic diagram of the drag reduction setup; (b) Relationship between shear rate and shear stress for SLIPS-1 and SLIPS-2. (c) Relationship between shear rate and viscosity for different samples. (d) Relationship between shear rate and drag reduction rate for different samples.

3.5. Anti-bacterial adhesion test

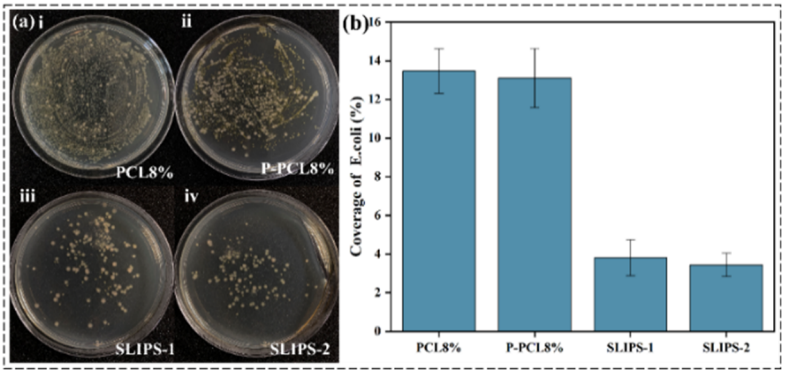

Figure 5. (a) Images of agar plates with diluted colonies of Escherichia coli after separation from the coating surface. (b) Escherichia coli surface coverage on the coating.

One prevalent marine Gram-negative bacteria is Escherichia coli. This study examined how different coatings affect E. coli adhesion using the plate method. Results showed that lubricant oil injection significantly reduced bacterial numbers on agar plates, enhancing the anti-adhesion rate. Figure 5 (a)

highlights this improvement. As shown in Figure 5 (b), non-oil-infused coatings (PCL8%, P-PCL8%) had up to 14.3% E. coli coverage, whereas oil-infused SLIPSs surfaces had only 2.86% coverage. This improvement is due to the lubricant layer preventing direct contact between bacteria and the surface, reducing adhesion and biofilm formation. The coating's antibacterial qualities are strengthened by the low interfacial energy between the lubricant and substrate, which also lowers adhesion rates[9].

4. Conclusion

The advantage of electrospinning technology lies in its highly controllable physical and chemical properties of the membrane. In this work, we generated porous PCL nanofibers based on optimal PCL processing parameters by means of non-solvent induced phase separation (NIPS). This resulted in improved lubricating oil storage stability, as well as drag reduction and marine anti-fouling benefits. With its rich porous structure, finer fiber diameter, and good internal connectivity, we can introduce active chemical substances with antibacterial properties in subsequent applications to achieve synergistic anti-fouling effects, providing a promising platform for marine anti-fouling.

Acknowledgments

This research was funded by the National Natural Science Foundation of China (Grant No. 52305605), the Natural Science Foundation of Jiangsu Higher Education Institutions of China (Grant No. 22KJB430022), and the Science Research Project of Jiangsu University of Science and Technology (Grant No. 1022932106).

References

[1] H. Palza, B. Barraza, F. Olate-Moya, An Overview for the Design of Antimicrobial Polymers: From Standard Antibiotic-Release Systems to Topographical and Smart Materials, Annu. Rev. Mater. Res. 52 (2022) 1–24. https://doi.org/10.1146/annurev-matsci-081720-105705.

[2] X. Liu, J.-L. Yang, D. Rittschof, J.S. Maki, J.-D. Gu, Redirecting marine antibiofouling innovations from sustainable horizons, Trends in Ecology & Evolution 37 (2022) 469–472. https://doi.org/10.1016/j.tree.2022.02.009.

[3] K.S. Grunnet, I. Dahllof, Environmental fate of the antifouling compound zinc pyrithione in seawater, Enviro Toxic and Chemistry 24 (2005) 3001–3006. https://doi.org/10.1897/04-627R.1.

[4] B. Anandkumar, R.P. George, C.J. Rao, J. Philip, In situ application of alternate potentials with chlorination synergistically enhanced biofouling control of titanium condenser materials, International Biodeterioration & Biodegradation 144 (2019) 104746. https://doi.org/10.1016/j.ibiod.2019.104746.

[5] D. Li, Z. Lin, Q. Liu, J. Zhu, J. Yu, J. Liu, Y. Wang, R. Chen, J. Wang, Lubricant-Infused Surface Enabled by Coral-like Microstructure Based on Flocking Powder and Its Anti-icing and Anticorrosion Performance, Ind. Eng. Chem. Res. 62 (2023) 13488–13497. https://doi.org/10.1021/acs.iecr.3c01666.

[6] Y. Guan, R. Chen, G. Sun, Q. Liu, J. Liu, J. Yu, C. Lin, J. Duan, J. Wang, The mussel-inspired micro-nano structure for antifouling:A flowering tree, Journal of Colloid and Interface Science 603 (2021) 307–318. https://doi.org/10.1016/j.jcis.2021.06.095.

[7] G. Zhang, P. Wang, X. Zhang, C. Xiang, L. Li, The preparation of PCL/MSO/SiO2 hierarchical superhydrophobic mats for oil-water separation by one-step method, European Polymer Journal 116 (2019) 386–393. https://doi.org/10.1016/j.eurpolymj.2019.04.011.

[8] S. Peppou-Chapman, J.K. Hong, A. Waterhouse, C. Neto, Life and death of liquid-infused surfaces: a review on the choice, analysis and fate of the infused liquid layer, Chem. Soc. Rev. 49 (2020) 3688–3715. https://doi.org/10.1039/D0CS00036A.

[9] Z. Yang, J. Chang, X. He, X. Bai, C. Yuan, Construction of robust slippery lubricant-infused epoxy-nanocomposite coatings for marine antifouling application, Progress in Organic Coatings 177 (2023) 107458. https://doi.org/10.1016/j.porgcoat.2023.107458.